JOURNAL OF SOLID STATE CHEMISTRY **127,** 87–91 (1996)
ARTICLE NO. 0360

Insulator–Metal Transitions, Giant Magnetoresistance, and Related Aspects of the Cation-Deficient $LaMnO_3$ Compositions $La_{1-\delta}MnO_3$ and $LaMn_{1-\delta'}O_3$

Anthony Arulraj,* R. Mahesh,* G. N. Subbanna,* R. Mahendiran,† A. K. Raychaudhuri,† and C. N. R. Rao*,[1]

*Solid State and Structural Chemistry Unit and †Department of Physics, Indian Institute of Science, Bangalore 560012 India

Received July 5, 1996; accepted August 14, 1996

Electron transport and magnetic properties of the cation-deficient compositions of $LaMnO_3$ with the nominal formulae $La_{1-\delta}MnO_3$ ($0.0 \leq \delta \leq 0.2$) and $LaMn_{1-\delta'}O_3$ ($0.0 \leq \delta' \leq 0.2$) were investigated after their defect structures were examined. $La_{1-\delta}MnO_3$ ($\delta = 0.1$) contains more than one defect structure involving both La and Mn vacancies. $La_{1-\delta}MnO_3$ ($0.0 \leq \delta \leq 0.2$) compositions are all ferromagnetic and show insulator–metal (I–M) transition, with the resistivity decreasing with increasing δ. $LaMn_{1-\delta'}O_3$ compositions show ferromagnetism and the I–M transition only up to $\delta' = 0.05$, with the resistivity increasing with δ'. All compositions showing the I–M transitions exhibit giant magnetoresistance.

INTRODUCTION

The discovery of giant magnetoresistance (GMR) in rare earth manganates of the type $Ln_{1-x}A_xMnO_3$ (*Ln*, rare earth; *A*, divalent cation) has created much interest in understanding the relation between structure and properties of these oxides (1–6). The substitution of La in $LaMnO_3$ by a divalent ion as in $La_{1-x}A_xMnO_3$ creates Mn^{4+}, around 30% Mn^{4+} being optimal for ferromagnetism and the associated insulator–metal (I–M) transition (4, 7). It has been shown recently that the proportion of Mn^{4+} in the parent $LaMnO_3$ itself can be varied by chemical or electrochemical means (8). Structural investigations of $LaMnO_3$ have revealed that Mn^{4+} ions are created in $LaMnO_3$ by the presence of vacancies in La and Mn sites, since excess oxygen cannot be accommodated in the close-packed perovskite structure (9–11). Furthermore, the La and Mn vacancies are present randomly and roughly in equal proportion in $LaMnO_3$. $LaMnO_3$ can tolerate a considerable proportion of vacancies in the A site (La), giving rise to compositions of the type $La_{1-\delta}MnO_3$ (12). We were interested in examining the structure, electron transport and magnetoresistance properties of cation-deficient compositions with vacancies in A or/and B sites. We have therefore studied the properties of manganates of nominal formulae $La_{1-\delta}MnO_3$ ($0.0 \leq \delta \leq 0.2$) and $LaMn_{1-\delta'}O_3$ ($0.0 \leq \delta' \leq 0.2$) where the vacancies are in the A and B sites, respectively. We show that while the vacancies in the B site are detrimental to ferromagnetism and the giant magnetoresistance, the A site can tolerate vacancies without destroying these properties.

EXPERIMENTAL

$La_{1-\delta}MnO_3$ and $LaMn_{1-\delta'}O_3$ ($0.0 \leq \delta$ or $\delta' \leq 0.2$) compositions were prepared by the sol–gel method by starting with the required quantities of La_2O_3 and $MnCO_3$ as the starting materials. Citric acid and ethylenediamine were used as gelling agents for the La and Mn ions in a nitrate solution. The gel thus obtained was decomposed and heated at 1223 K for 48 h. The Mn^{4+} content of the samples was determined by redox titrations using standard potassium permanganate and ferrous sulfate solutions. Thermogravimetric analysis has been carried out using CAHN TG 131 thermogravimetric analyzer.

Powder X-ray diffraction patterns recorded on a JEOL. JDX-8P diffractometer with Cu$K\alpha$ radiation were used to check the phase purity and to determine the unit cell parameters of various compositions. A JEOL 3010 transmission electron microscope (TEM) fitted with an ultra-high resolution objective pole piece (~1.7 Å point to point resolution) was used for ultramicrostructure studies. Specimens for electron microscopy were prepared by both suspending the fine powder in an organic solvent on holey carbon grids as well as by Ar-ion beam thinning of 3-mm discs cut from sintered pellets using a Gatan Duomill.

Electrical resistivity measurements were performed in the temperature range 4.2–300 K using the standard four-probe technique. Magnetoresistance measurements were carried out in the same temperature range up to a field of

[1] To whom the correspondence should be addressed.

0022-4596/96 $18.00

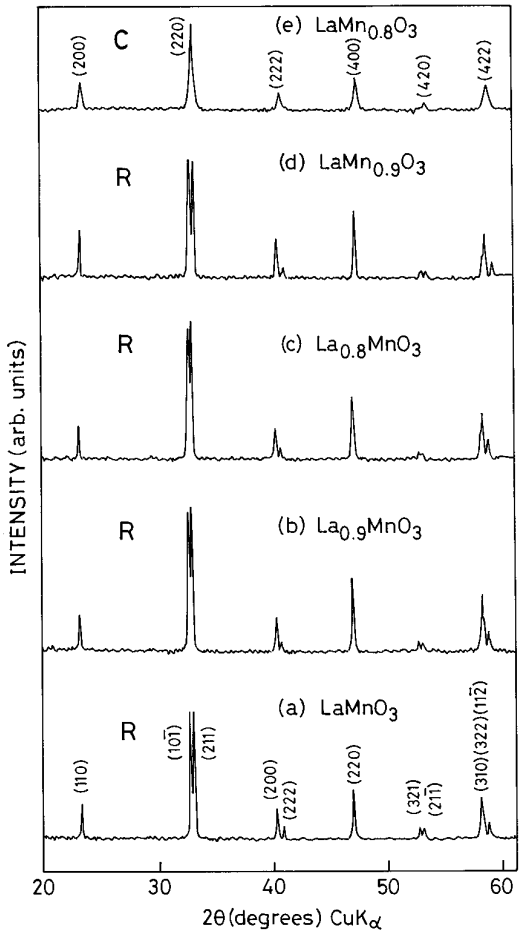

FIG. 1. Powder X-ray diffraction patterns of $La_{1-\delta}MnO_3$ and $LaMn_{1-\delta'}O_3$ compositions.

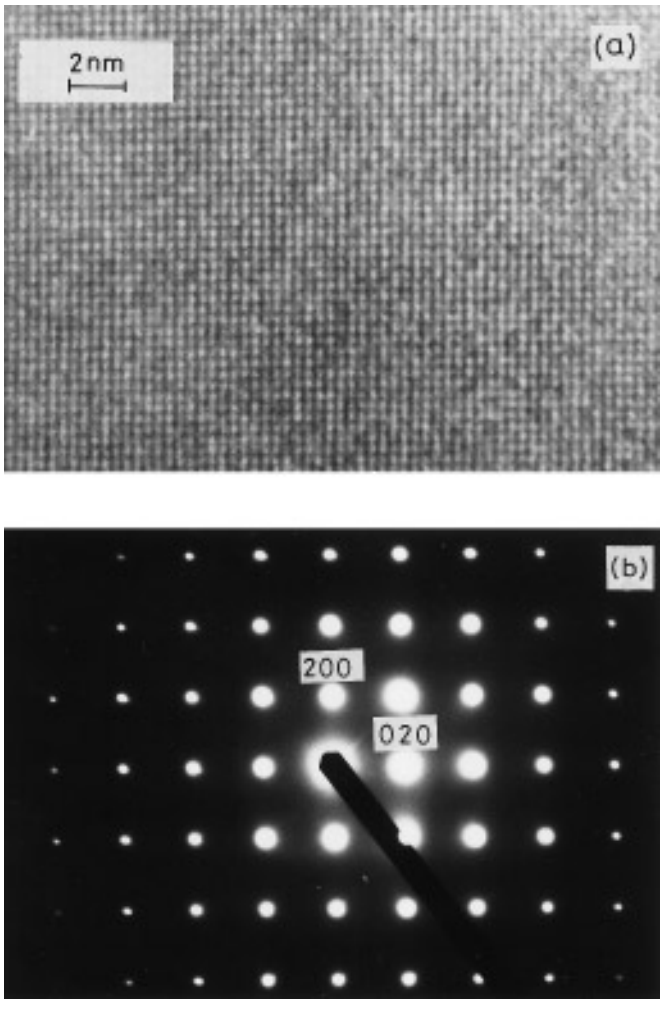

FIG. 2. (a) High-resolution electron microscopic image of $La_{0.9}MnO_3$ in the [001] orientation. Notice the regular contrast in the image. (b) The corresponding SAED pattern.

6 T using a superconducting solenoid. Magnetic susceptibility (ac) was measured with a mutual inductance bridge operating at 100 Hz in an ac magnetic field less than 5 mT so that the measured susceptibility was in the range of reversible magnetization.

RESULTS AND DISCUSSION

In Fig. 1, we show the powder X-ray diffraction patterns of the $La_{1-\delta}MnO_3$ and $LaMn_{1-\delta'}O_3$ compositions. The $La_{1-\delta}MnO_3$ compositions up to $\delta = 0.2$ have the rhombohedral structure ($R\bar{3}c$ with $a = \sqrt{2}\, a_p$ and $\alpha \approx 60°$) with the unit cell parameters listed in Table 1. The parent $LaMnO_3$ as prepared by the sol–gel method has 26% Mn^{4+}. By heating the sample in a N_2 atmosphere at 1173 K or in air at higher temperatures, we obtain $LaMnO_3$ samples with ~10% or less of Mn^{4+}. It is noteworthy that with increasing δ, the Mn^{4+} content decreases in $La_{1-\delta}MnO_3$. This can happen if there is some oxygen deficiency, although these compositions were prepared by gel route in oxygen atmosphere to avoid the oxygen deficiency as much as possible. The $LaMn_{1-\delta'}O_3$ compositions are rhombohedral up to $\delta' = 0.1$ and become pseudocubic with $\delta' = 0.05$ or 0.20. The Mn^{4+} content of $LaMn_{1-\delta'}O_3$ increases with δ'.

Based on the Mn^{4+} content obtained by redox titrations, we derive the approximate compositions of the $\delta = 0.0, 0.1$, 0.2 and $\delta' = 0.1$ and 0.2 compositions to be $La_{0.96}Mn_{0.96}O_3$, $La_{0.9}MnO_{2.96}$, $La_{0.8}MnO_{2.79}$, and $La_{0.99}Mn_{0.89}O_3$ and $LaMn_{0.8}O_{2.932}$, respectively, assuming equal proportion of vacancies in excess of the nominal compositions on the A and B sites (11). In order to understand the defect structure, we carried out thermogravimetric analysis of the $\delta = 0.0, 0.1$ and $\delta' = 0.1$ samples in a H_2/N_2 mixture (20 : 80 by molar volume). The observed weight losses were 4.1,

TABLE 1
Properties of $La_{1-\delta}MnO_3$ and $LaMn_{1-\delta'}O_3$

Nominal composition		Mn^{4+}	Structure[a]	Lattice parameter		T_c (K)	T_p (T_p^*)[c] (K)	−MR (%)
				a (Å)	α (°)			
δ	0.00	26	R	5.461	60.42	230	200 (000)	52
	0.05	24	R	5.460	60.46	—[b]	220 (235)	—[b]
	0.10	22	R	5.460	60.48	278	242 (250)	50
	0.15	21	R	5.457	60.48	—[b]	240 (260)	—[b]
	0.20	19	R	5.462	60.49	268	240 (260)	—[b]
δ'	0.05	19	R	5.453	60.53	224	175	65
	0.10	39	R	5.437	60.86	—	—	—
	0.15	51	C	7.754	—	—	—	—
	0.20	58	C	7.732	—	—	—	—

[a] R, rhombohedral; C, pseudocubic.
[b] Not measured.
[c] Those compositions for which T_p is not mentioned are insulating. T_p^* refers to the temperature corresponding to the shoulder in the resistivity.

5.2, and 5.34% for the $\delta = 0.0$, 0.1 and $\delta' = 0.1$, respectively (at 1173 K), the final products being La_2O_3 and MnO. The observed weight loss in the $\delta = 0.0$ samples is close to that expected from the formula $La_{0.96}Mn_{0.96}O_3$ (obtained from redox titration). The observed values of the weight loss are, however, higher than the expected values for the samples of the nominal formulae of $La_{0.9}MnO_3$ and $LaMn_{0.9}O_3$, suggesting that there is some oxygen deficiency. We are not able to fix the exact defect formulae of $La_{0.9}MnO_3$ and $LaMnO_{0.9}O_3$ because we have only two experimentally observed quantities (Mn^{4+} content and the weight loss) and there are three unknowns (δ, δ', and the oxygen deficiency). We should note here that for a given nominal composition such as $La_{0.9}MnO_3$, more than one defect composition can, in principle, occur together, since the crystal lattice can accommodate such variations.

In order to examine the defect structure of $La_{1-\delta}MnO_3$ and $LaMn_{1-\delta'}O_3$, we have carried out high-resolution electron microscopic (HREM) studies along with selected area electron diffraction. The electron diffraction patterns of $La_{0.9}MnO_3$ recorded from various grains along [001] as well as other directions could be indexed with respect to a face-centered rhombohedral cell with $a \approx 2 \times a_p$ and $\gamma \approx 90°$ ($a_p \approx 3.9$ Å). The [001] HREM images of the specimens show regular contrast in the grain without any defects or disorder structure. A typical image recorded is shown with the corresponding selected area diffraction pattern in Figs. 2a and 2b. A careful examination of Ar-ion thinned specimen showed fine precipitation of faceted regions close to grain boundaries. We show a bright-field image recorded from such a region in Fig. 3a. The regions located along the grain boundaries have diameters less than 400 Å. The lattice image of one such region is shown in Fig. 3b. The fringe spacing observed is about 2.5 Å. From the morphology and the lattice image, we believe that these regions correspond to a cubic phase nucleated in the rhombohedral grains, $La_{1-\delta}MnO_3$ preferentially along the grain boundaries. In other words $La_{0.9}MnO_3$ (nominal composition) is actually composed of at least two defect compositions, $La_{1-\delta 1}Mn_{1-\delta 1'}O_3$ (rhombohedral) and $La_{1-\delta 2}Mn_{1-\delta 2'}O_3$ (pseudocubic). Earlier studies from this laboratory (11) had shown that compositions of $LaMnO_3$ with around 33% of Mn^{4+} have a cubic structure with the approximate composition $La_{0.945}Mn_{0.945}O_3$. Presence of more than one defect composition in such oxides cannot be readily detected by powder X-ray diffraction patterns. Unlike $La_{0.9}MnO_3$, $LaMn_{0.9}O_3$ does not reveal the presence of more than one defect composition in HREM images. Instead, the images show regular contrast. HREM images of both $La_{0.9}MnO_3$ and $LaMn_{0.9}O_3$ do not show extended defects. The La as well as Mn vacancies are therefore likely to be distributed randomly as suggested earlier (9–11).

We show the temperature variation of the ac magnetic susceptibility of the various $La_{1-\delta}MnO_3$ compositions in Fig. 4. The measurements show the $\delta = 0.0$, 0.1, and 0.2 compositions to be ferromagnetic with T_c values of 230, 273, and 268 K, respectively. In the case of $LaMn_{1-\delta'}O_3$, only the $\delta' = 0.05$ composition shows a ferromagnetic transition with a T_c of 224 K (Fig. 5). $LaMn_{0.9}O_3$ ($\delta' = 0.1$) does not show ferromagnetism. It appears that even 10% vacancies at the B site destroys ferromagnetism in these manganates. This is not entirely surprising as the Mn ions are directly involved in determining the magnetic properties of these manganates.

In Fig. 6a, we show the temperature variation of the electrical resistivity of $La_{1-\delta}MnO_3$ compositions. All of

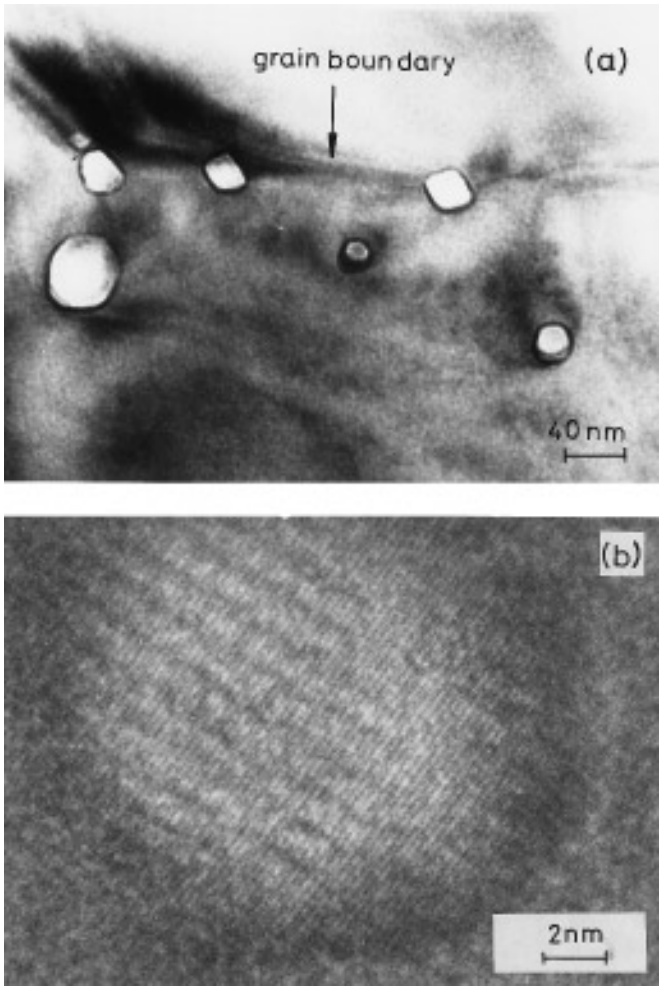

FIG. 3. (a) Bright-field image of $La_{0.9}MnO_3$ (Ar-ion beam thinned sample). (b) Lattice image of one of the faceted particles of $La_{0.9}MnO_3$.

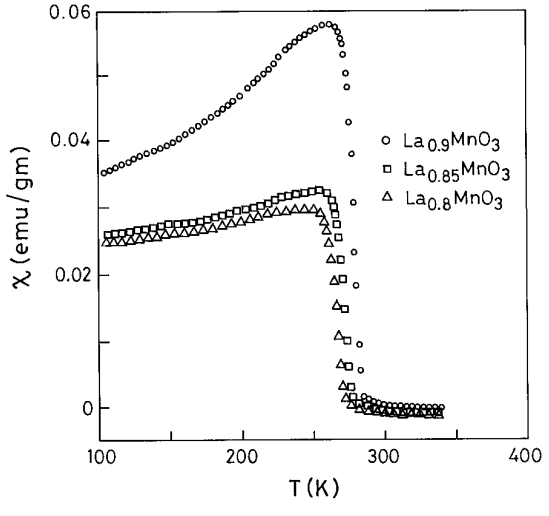

FIG. 4. Temperature variation of magnetic susceptibility data of $La_{1-\delta}MnO_3$ ($\delta = 0.1, 0.15, 0.2$).

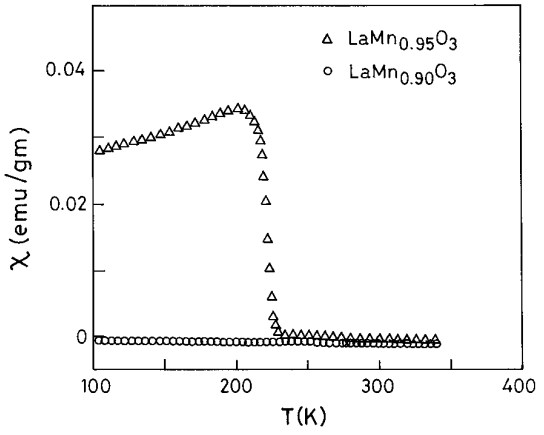

FIG. 5. Temperature variation of magnetic susceptibility data of $LaMn_{1-\delta'}O_3$ ($\delta' = 0.05, 0.1$).

them show insulator–metal transitions with a maximum in resistivity. The resistivity plots show a major peak and a shoulder in samples with $\delta > 0.0$. The temperature corresponding to the maximum in resistivity (T_p) increases with increasing δ. The resistivity, especially at T_p, decreases with increase in δ. The appearance of double maxima in the resistivity curve in Fig. 6a suggests the coexistence of two similar phases. We suggest that these are due to the presence of more than one defect compositions discussed earlier, which cannot be detected by X-ray diffraction.

In Fig. 6b, we show the temperature variation of the electrical resistivity of the $LaMn_{1-\delta'}O_3$ compositions. Only the $\delta' = 0.05$ composition which is ferromagnetic shows the transition (~175 K) and the T_p is slightly lower than that of $\delta' = 0.0$. The resistivity increases with δ' and the $\delta' = 0.1$ composition is insulating. It may be recalled that the $\delta' = 0.1$ compositions did not show a ferromagnetic transition as well. Since both the ferromagnetism and the

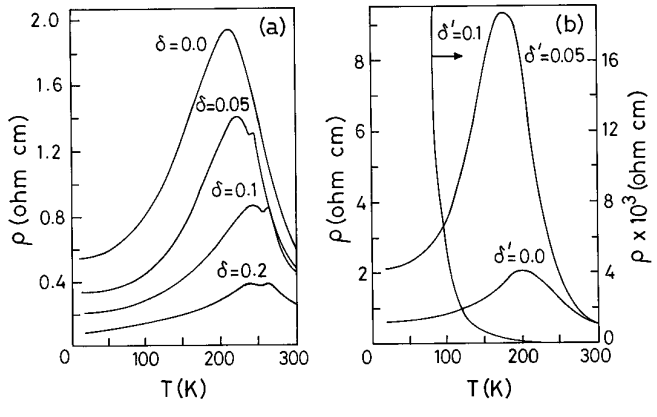

FIG. 6. Variation of the electrical resistivity with temperature in (a) $La_{1-\delta}MnO_3$ and (b) $LaMn_{1-\delta'}O_3$.

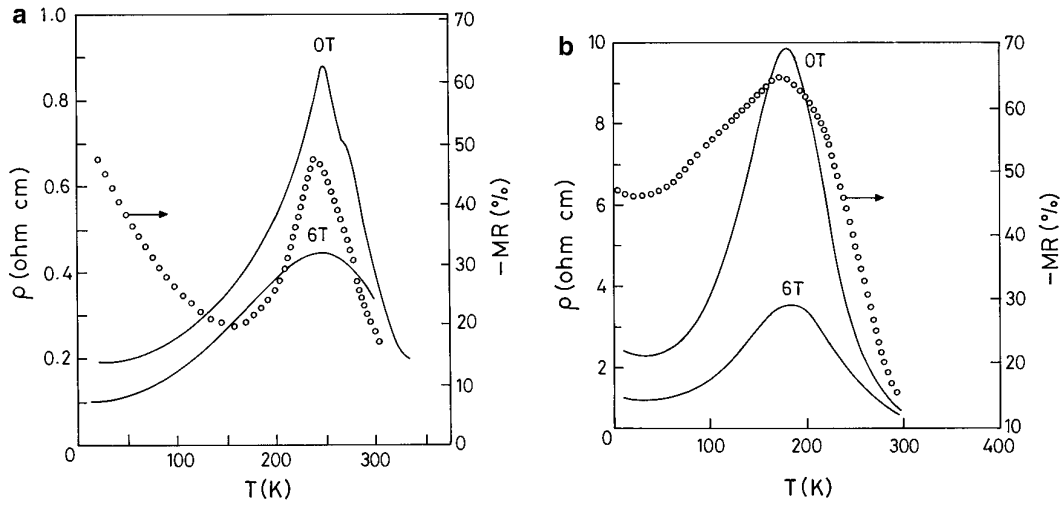

FIG. 7. Temperature variation of electrical resistivity (at $H = 0$ and 6 T) and magnetoresistance in (a) $La_{0.9}MnO_3$ and (b) $LaMn_{0.95}O_3$.

electrical conductivities are determined by the double-exchange mechanism operative in the manganates, we would expect vacancies at the B site to destroy the ferromagnetism accompanied by an increase in resistivity.

In Figs. 7a and 7b, we show the resistivity data of the $La_{0.9}MnO_3$ and $LaMn_{0.95}O_3$ compositions, respectively, at 0 and 6 T. We observe a significant decrease in resistivity at T_p on the application of the magnetic field in both the cases. The magnitude of magnetoresistance is maximum at T_p. The magnetoresistance in $La_{0.9}MnO_3$ and $LaMn_{0.95}O_3$ are 50 and 65% respectively at T_p. The magnitude of magnetoresistance does not show a monotonic dependence on temperature and goes to a limiting value as $T \rightarrow 4.2$ K. $LaMn_{1-\delta'}O_3$ compositions with $\delta' > 0.05$, which do not exhibit ferromagnetism as well as the I–M transition, did not show appreciable MR. In Table 1, we list the T_c, T_p, and other properties of $La_{1-\delta}MnO_3$ and $LaMn_{1-\delta'}O_3$ compositions.

ACKNOWLEDGMENT

The authors thank the Indo-French Centre for Advanced Research, Department of Science and Technology and the CSIR for support.

REFERENCES

1. K. Chahara, T., Ohno, M. Kasai, and Y. Kozono, *Appl. Phys. Lett.* **63,** 1990 (1993).
2. R. Von Helmolt, J. Wecker, B. Holzapfel, L. Schultz, and K. Samner, *Phys. Rev. Lett.* **71,** 2331 (1993).
3. A. Urushibara, Y. Moritomo, T. Arima, A. Asamitsu, G. Kido, and Y. Tokura, *Phys. Rev. B* **51,** 14103 (1995).
4. R. Mahendiran, R. Mahesh, N. Rangavittal, S. K. Tiwari, A. K. Raychaudhuri, T. V. Ramakrishnan, and C. N. R. Rao, *Phys. Rev. B* **53,** 3348 (1996).
5. B. Raveau, A. Maignan, and V. Caignaert, *J. Solid State Chem.* **117,** 424 (1995).
6. H. L. Ju, J. Gopalakrishnan, J. L. Peng, Q. li, G. C. Xiong, T. Venkatesan, and R. L. Greene, *Phys. Rev. B* **51,** 6143 (1995).
7. G. H. Jonker and J. H. van Santen, *Physica* **16,** 337 (1950).
8. M. Verelst, N. Rangavittal, C. N. R. Rao, and A. Rousset, *J. Solid State Chem.* **74,** 104 (1993); R. Mahesh, K. R. Kannan, and C. N. R. Rao, *J. Solid State Chem.* **114,** 294 (1995).
9. J. A. M. van Roosmalen, E. H. P. Cordfunke, R. B. Helmholdt, and H. W. Zandbergen, *J. Solid State Chem.* **110,** 100 (1994).
10. J. A. M. van Roosmalen and E. H. P. Cordfunke, *J. Solid State Chem.* **110,** 109 (1994).
11. M. Hervieu, R. Mahesh, N. Rangavittal and C. N. R. Rao, *Eur. J. Solid State Inorg. Chem.* **32,** 79 (1995).
12. V. Ferris, L. Brohan, M. Ganne, and M. Tournoux, *Eur. J. Solid State Inorg. Chem.* **32,** 131 (1995).